PSI TR-34

ADVANCED REENTRY AEROMECHANICS
INTERIM SCIENTIFIC REPORT

VOLUME I

A REYNOLDS STRESS MODEL FOR BOUNDARY LAYER TRANSITION WITH APPLICATION TO ROUGH SURFACES

M. L. FINSON

August 1975

Jointly Sponsored by

The Space and Missile Systems Organization
and
The Air Force Office of Scientific Research (AFSC)
Contract F44620-74-C-0022

PHYSICAL SCIENCES INC.
18 LAKESIDE OFFICE PARK, WAKEFIELD, MASSACHUSETTS

"Qualified requestors may obtain additional copies from the Defense Documentation Center, all others should apply to the National Technical Information Service."

UNCLASSIFIED

SECURITY CLASSIFICATION OF THIS PAGE (When Data Entered)

REPORT DOCUMENTATION PAGE

READ INSTRUCTIONS BEFORE COMPLETING FORM

REPORT NUMBER	2. GOVT ACCESSION NO. / 3. RECIPIENT'S CATALOG NUMBER
4. TITLE (and Subtitle): Advanced Reentry Aeromechanics. Volume I. A REYNOLDS STRESS MODEL FOR BOUNDARY LAYER TRANSITION WITH APPLICATION TO ROUGH SURFACES. ~~Volume I.~~	TYPE OF REPORT & PERIOD COVERED: INTERIM Scientific Rept. 1 Jul [illegible]74 — 30 Jun [illegible]75 / PSI-TR-34
7. AUTHOR(s): MICHAEL L. FINSON	CONTRACT OR GRANT NUMBER(s): F44620-74-C-0022
9. PERFORMING ORGANIZATION NAME AND ADDRESS: PHYSICAL SCIENCES INC. 18 Lakeside Office Park Wakefield, MA 01880	10. PROGRAM ELEMENT, PROJECT, TASK AREA & WORK UNIT NUMBERS: 681307 / AF-9781-03 / 61102F / 1781Ø3
11. CONTROLLING OFFICE NAME AND ADDRESS: AIR FORCE OFFICE OF SCIENTIFIC RESEARCH/NA BUILDING 410 BOLLING AIR FORCE BASE, D C 20332	12. REPORT DATE: Aug [illegible]75 / 13. NUMBER OF PAGES: 42 / 47Ø
14. MONITORING AGENCY NAME & ADDRESS(if different from Controlling Office)	15. SECURITY CLASS. (of this report): Unclassified / 15a. DECLASSIFICATION/DOWNGRADING SCHEDULE

16. DISTRIBUTION STATEMENT (of this Report)

Approved for public release; distribution unlimited.

17. DISTRIBUTION STATEMENT (of the abstract entered in Block 20, if different from Report)

18. SUPPLEMENTARY NOTES

19. KEY WORDS (Continue on reverse side if necessary and identify by block number)

BOUNDARY LAYER TRANSITION
TURBULENT BOUNDARY LAYERS
TRANSITION PREDICTIONS
SURFACE ROUGHNESS

20. ABSTRACT (Continue on reverse side if necessary and identify by block number)

A theory based on the use of second-order moment equations is presented for transitional and turbulent boundary layer flows. The technique yields accurate predictions for various fully turbulent boundary layers, including those affected by pressure gradients and surface roughness. Although the model has yet to be adequately developed for treating transition induced by free-stream turbulence, a method is presented that addresses wall-roughness dominated transition. Using an idealized reprecti-

DD FORM 1 JAN 73 1473 EDITION OF 1 NOV 65 IS OBSOLETE

UNCLASSIFIED

SECURITY CLASSIFICATION OF THIS PAGE (When Data Entered)

391105

tation of distributed roughness elements, the disturbances introduced by the elements are described by wake relations and are handled as distributed source or sink terms in the governing relations for mean momentum and fluctuating energy. Representation of actual roughness distributions should be feasible in computations performed with this model. The effects of roughness size and shape on transition are evaluated, and transition is found to be most sensitive to the location of the peaks of the roughness elements. Calculations performed to date compare satisfactorily with the transition measurements of Feindt[27] on sand paper-roughened flat plates in low speed flow.

PSI TR-34

ADVANCED REENTRY AEROMECHANICS
INTERIM SCIENTIFIC REPORT

VOLUME I

A REYNOLDS STRESS MODEL FOR BOUNDARY LAYER TRANSITION WITH APPLICATION TO ROUGH SURFACES

M. L. FINSON

August 1975

Jointly Sponsored by

The Space and Missile Systems Organization

and

The Air Force Office of Scientific Research (AFSC)

Contract F44620-74-C-0022

PHYSICAL SCIENCES INC.
18 Lakeside Office Park
Wakefield, Massachusetts 01880

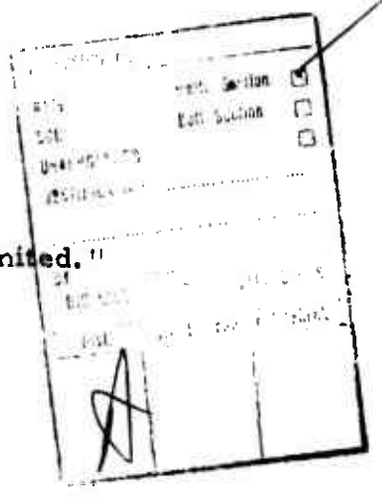

Conditions of Reproduction

ABSTRACT

A theory based on the use of second-order moment equations is presented for transitional and turbulent boundary layer flows. The technique yields accurate predictions for various fully turbulent boundary layers, including those affected by pressure gradients and surface roughness. Although the model has yet to be adequately developed for treating transition induced by free-stream turbulence, a method is presented that addresses wall-roughness dominated transition. Using an idealized representation of distributed roughness elements, the disturbances introduced by the elements are described by wake relations and are handled as distributed source or sink terms in the governing relations for mean momentum and fluctuating energy. Representation of actual roughness distributions should be feasible in computations performed with this model. The effects of roughness size and shape on transition are evaluated, and transition is found to be most sensitive to the location of the peaks of the roughness elements. Calculations performed to date compare satisfactorily with the transition measurements of Feindt[27] on sand paper-roughened flat plates in low speed flow.

ACKNOWLEDGEMENTS

Sponsorship Statement

Research jointly sponsored by the Space and Missile Systems Organization and the Air Force Office of Scientific Research (AFSC), United States Air Force, under Contract F44620-74-C-0022. The United States Government is authorized to reproduce and distribute reprints for governmental purposes notwithstanding any copyright notation hereon.

The author is indebted to Mr. Paul F. Lewis for the development and implementation of the numerical techniques used in this study.

TABLE OF CONTENTS

LIST OF ILLUSTRATIONS

1. INTRODUCTION

Boundary layer transition and the ensuing turbulent heat transfer is an important consideration in the design of high performance reentry vehicle nosetips. Transitional heat transfer can bring about complicated changes in nose shape, with frequently undesirable aerodynamic vehicle performance. This report describes the results of an effort to construct fundamental methods for predicting the development of nosetip boundary layers. Such flows are obviously quite complex-compressibility, entropy swallowing, pressure gradients, mass transfer, and surface roughness are often important. Our objectives include the prediction of transition as well as the subsequent increases in heating rate through the transitional and turbulent zones.

The technical approach for this study is based on solving the governing equations for various fluctuating intensities, derived by a technique often referred to as "second-order closure". Recent years have seen considerable development of second-order closure methods for treating turbulent flows, and the model presented here has been successfully applied to a variety of flows including boundary layers, wakes, mixing layers, etc. However, the application to transition is rather new.

Figure 1 is a schematic representation of the transition process, plotting the fluctuation intensity, heat transfer rate or other such parameter against Reynolds number. The true behavior starts from a low level, amplifies, and typically exhibits a mild overshoot before reaching fully-developed turbulent values. Given the appropriate initial disturbances, linear stability theory should describe the initial stages of development accurately but would continue to show amplification without limit. A

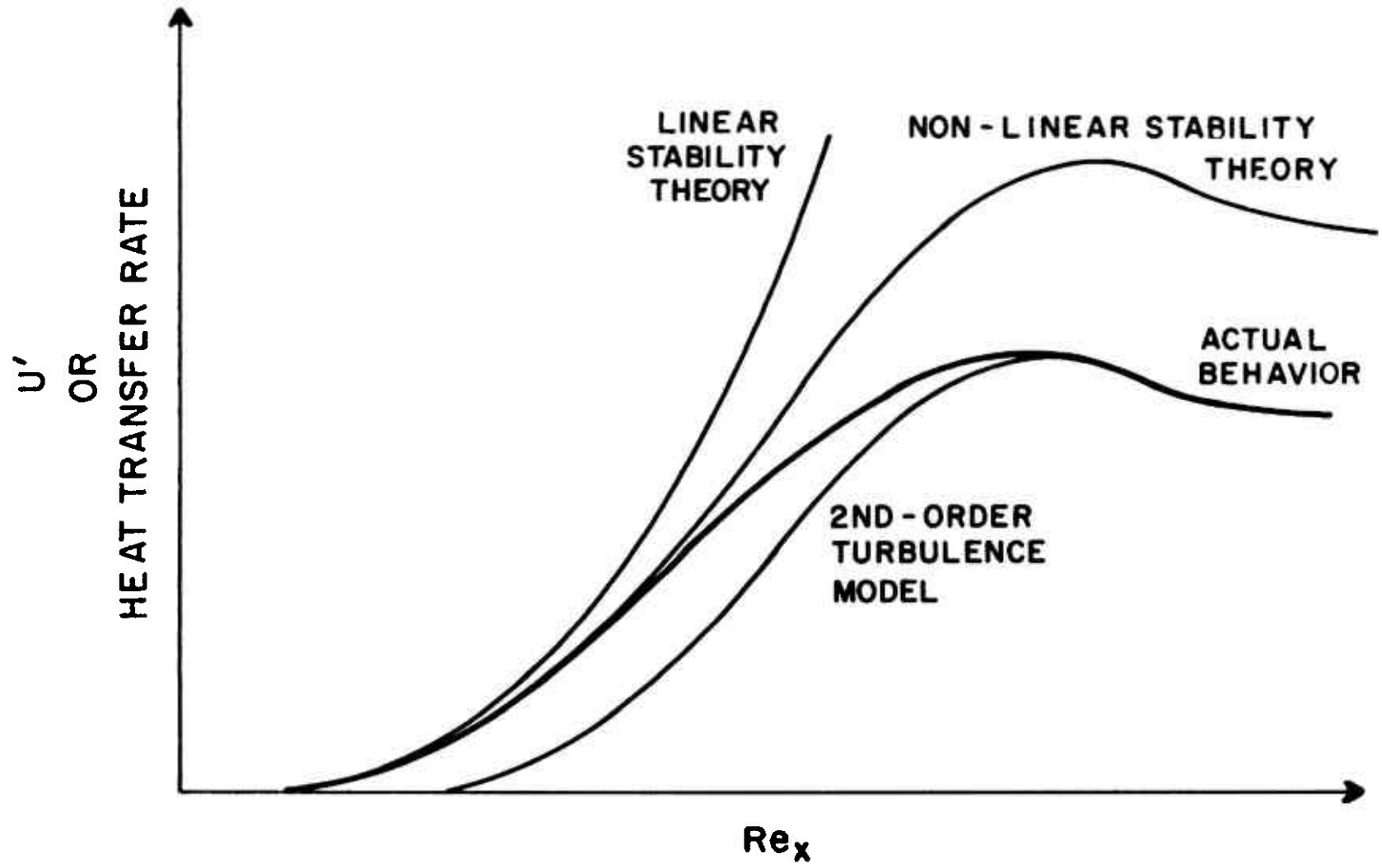

Fig. 1 Schematic of Transitional
Boundary Layer Development

nonlinear stability theory (which has not been formulated for boundary layers) would include the dissipative effects that limit amplification but would probably not yield accurate answers in the final stages unless the theory accounted for the development of a continuous turbulent spectrum. A second-order turbulence model, on the other hand, should become increasingly valid as turbulent intensities build up. And, if the model contains the appropriate low Reynolds number terms, it may be useful at the earlier stages.

The basic model development was described in a previous report,[1] and will be summarized in the following section. Results for smooth-wall boundary layers will be discussed briefly in the third section. However, the major emphasis of this effort has concerned the behavior of boundary layers over rough walls. At low altitudes, nosetip boundary layers are usually so thin that surface roughness plays a dominant role. The fourth section presents a model for the manner by which surface roughness introduces disturbances into a boundary layer, and the fifth section describes results for transition on rough walls.

II. SECOND-ORDER CLOSURE MODEL

The development of the model used in this study has been described in detail elsewhere,[1,2] and only the results shall be presented here. Our treatment of closure draws upon aspects of various previous work, most notably Rotta's treatment of low Reynolds number effects[3] and the description by Hanjalic and Launder[4] of the triple fluctuation and pressure fluctuation terms. Wherever possible, closure approximations have been evaluated against basic laboratory experiments (e.g. grid turbulence), the types of experiments being chosen to attempt to isolate individual terms.

The formulation accounts for both mean and fluctuating velocity and temperature quantities. The dependent velocity variables are the mean velocity vector U_i, the Reynolds stress tensor $\overline{u_i' u_j'}$, and the isotropic dissipation rate Φ; under the boundary layer approximation this set of variables reduces to $U, V, \overline{u'^2}, \overline{v'^2}, \overline{w'^2}, \overline{u'v'}$, and Φ. In practice it is convenient to replace $\overline{u'^2}$, $\overline{v'^2}$, $\overline{w'^2}$ by the kinetic energy $q^2 = (\overline{u'^2} + \overline{v'^2} + \overline{w'^2})/2$ and two measures of the degree of anisotropy $S_{11} = \overline{u'^2} - 2/3\, q^2$, $S_{22} = \overline{v'^2} - 2/3\, q^2$.

For steady flow the governing equations include continuity:

$$\frac{\partial}{\partial x_i} (\rho U_i) = 0 \tag{1}$$

the mean momentum equation:

$$\rho U_k \frac{\partial U}{\partial x_k} = - \frac{\partial \bar{p}}{\partial x} - \frac{\partial}{\partial y} (\rho \overline{uv}) + \frac{\partial}{\partial y} (\mu \frac{\partial U}{\partial y}) \tag{2}$$

and, for the five second-order quantities:

$$\rho U_k \frac{\partial q^2}{\partial x_k} = -\rho \overline{uv} \frac{\partial U}{\partial y} - \rho \Phi + 0.15 \frac{\partial}{\partial y}\left[\rho \frac{q^2 v^2}{\Phi} \frac{\partial}{\partial y}(q^2 + v^2)\right]$$

$$+ \frac{\partial}{\partial y} \mu \frac{\partial q^2}{\partial y} + (S_{22} - S_{11}) \rho \frac{\partial U}{\partial x} \tag{3}$$

$$\rho U_k \frac{\partial S_{11}}{\partial x_k} = -\frac{14}{33} \rho \overline{uv} \frac{\partial U}{\partial y} - C_E \rho \frac{\Phi}{q^2} S_{11} + 0.15 \frac{\partial}{\partial y}\left[\rho \frac{q^2 v^2}{\Phi} \frac{\partial}{\partial y}(S_{11} - \frac{2}{3} v^2)\right]$$

$$+ \frac{\partial}{\partial y} \mu \frac{\partial S_{11}}{\partial y} - \rho \left[\frac{8}{15} q^2 + \frac{2}{33} S_{11} + \frac{1}{33} S_{22}\right] \frac{\partial U}{\partial x} \tag{4}$$

$$\rho U_k \frac{\partial S_{22}}{\partial x_k} = \frac{13}{33} \rho \overline{uv} \frac{\partial U}{\partial y} - C_E \rho \frac{\Phi}{q^2} S_{22} + 0.15 \frac{\partial}{\partial y}\left[\rho \frac{q^2 v^2}{\Phi} \frac{\partial}{\partial y}(S_{22} - \frac{4}{3} v^2)\right]$$

$$+ \frac{\partial}{\partial y} \mu \frac{\partial S_{22}}{\partial y} + \rho \left[\frac{8}{15} q^2 + \frac{1}{33} S_{11} + \frac{2}{33} S_{22}\right] \frac{\partial U}{\partial x} \tag{5}$$

$$\rho U_k \frac{\partial \overline{uv}}{\partial x_k} = -\rho \left[\frac{4}{15} q^2 - \frac{2}{11} S_{11} + \frac{5}{22} S_{22}\right] \frac{\partial U}{\partial y} - C_E \rho \frac{\Phi}{q^2} \overline{uv}$$

$$+ 0.30 \frac{\partial}{\partial y}\left[\rho \frac{q^2 v^2}{\Phi} \frac{\partial \overline{uv}}{\partial y}\right] + \frac{\partial}{\partial y} \mu \frac{\partial \overline{uv}}{\partial y} \tag{6}$$

$$\rho U_k \frac{\partial \Phi}{\partial x_k} = -1.25\,\rho \frac{\overline{uv}}{q^2} \frac{\partial U}{\partial y}\Phi - C_\Phi \rho \frac{\Phi^2}{q^2} + 14.8\,\rho \frac{\nu q^2}{\Phi y^2}$$

$$+ 0.15 \frac{\partial}{\partial y}\left[\rho \frac{q^2 v^2}{\Phi} \frac{\partial \Phi}{\partial y}\right] + \frac{\partial}{\partial y}\mu \frac{\partial \Phi}{\partial y} - 1.25\,\rho \frac{u^2}{q^2} \frac{\partial U}{\partial x}\Phi \qquad (7)$$

where $C_E = \dfrac{1.2 + 12.5\,\pi/Re_\Lambda}{1 + 12.5\,\pi/Re_\Lambda}$, $C_\Phi \dfrac{0.288 + 6.6\,\pi/Re_\Lambda + 35\,\pi^2/Re_\Lambda^2}{(0.4 + 5\,\pi/Re_\Lambda)^2}$

and Re_Λ is the turbulent Reynolds number $q\,\Lambda/\nu$, with Λ being related to the dissipation rate by

$$\Phi = 0.4 \frac{q^3}{\Lambda} + 5\,\pi\,\nu \frac{q^2}{\Lambda^2} = 0.4 \frac{q^3}{\Lambda}\,(1 + 12.5\,\pi/Re_\Lambda) \qquad (8)$$

It may be noted that, in the limit $Re_\Lambda \to \infty$, Eqs. (1) - (7) are somewhat similar to those derived by Launder et al.[4,5] However, low Reynolds number effects are also included here, in the molecular diffusion terms and in the Re_Λ dependence of the sink terms involving C_E and C_Φ. The term $14.8\,\rho\nu\,q^2/(\Phi\,y^2)$ is a "wall term", required to obtain a well-behaved solution in the viscous sublayer, $y \to 0$ (a somewhat different but equivalent term was used in Ref. 1)*

* Launder et al.[5] have recently proposed inclusion of additional wall terms that would contribute in the logarithmic region of a fully-turbulent boundary layer. We have yet to evaluate such terms, although it appears that their overall effect may not be major. Of more importance may be the viscous sublayer. The present formulation guarantees that turbulent intensities decay sufficiently rapidly as $y \to 0$, but more accurate descriptions of the actual processes that occur in the sublayer may be possible.

For high speed flows it is also necessary to describe the temperature or enthalpy field. The mean temperature is required to determine density and the Reynolds heat flux $\overline{v' T'}$ is of primary interest for heat transfer considerations. To accomplish this we include as additional dependent variables the mean static enthalpy $\bar{h}$, the mean-square fluctuating enthalpy $\overline{h'^2}$, and the transverse and axial components of the Reynolds heat flux $\overline{v' h'}$ and $\overline{u' h'}$. Required closure approximations have been carried out in a manner analogous to those leading to the velocity equations above, although the paucity of measurements of fluctuating temperatures has made it difficult to completely verify closure approximations against basic laboratory data. The resulting enthalpy equations are:

$$\rho \frac{D\bar{h}}{Dt} = \overline{U_i} \frac{\partial \bar{p}}{\partial x_i} - \frac{\partial}{\partial y}\left(\rho \overline{v' h'}\right) + \frac{1}{Pr} \frac{\partial}{\partial y}\left(\mu \frac{\partial \bar{h}}{\partial y}\right) + \mu\left(\frac{\partial U}{\partial y}\right)^2 + \rho \Phi \tag{9}$$

$$\rho \frac{D\overline{h'^2}}{Dt} = -2\rho \overline{v' h'} \frac{\partial \bar{h}}{\partial y} - C_{T_1} \rho \frac{\Phi}{q^2} \overline{h'^2} + 0.40 \frac{\partial}{\partial y}\left(\rho \frac{q^2 v^2}{\Phi} \frac{\partial \overline{h'^2}}{\partial y}\right) + \frac{1}{Pr} \frac{\partial}{\partial y}\left(\mu \frac{\partial \overline{h'^2}}{\partial y}\right) \tag{10}$$

$$\rho \frac{D\overline{v' h'}}{Dt} = -\rho v^2 \frac{\partial \bar{h}}{\partial y} - 0.09835\, \bar{\rho}\, \overline{u' h'} \frac{\partial U}{\partial y} - C_{T_2} \rho \frac{\Phi}{q^2} \overline{v' h'} + 0.80 \frac{\partial}{\partial y}\left(\rho \frac{q^2 v^2}{\Phi} \frac{\partial}{\partial y} \overline{v' h'}\right) + \frac{1}{Pr} \frac{\partial}{\partial y}\left(\mu \frac{\partial v' h'}{\partial y}\right) \tag{11}$$

$$\rho \frac{D\overline{u'h'}}{Dt} = -0.3989\,\rho\,\overline{v'h'}\,\frac{\partial U}{\partial y} - \rho\,\overline{uv}\,\frac{\partial \bar{h}}{\partial y} - C_{T_2}\,\rho\,\frac{\Phi}{q^2}\,\overline{u'h'}$$

$$+ 0.40\,\frac{\partial}{\partial y}\left(\rho\,\frac{q^2 v^2}{\Phi}\,\frac{\partial \overline{u'h'}}{\partial y}\right) + \frac{1}{Pr}\,\frac{\partial}{\partial y}\left(\mu\,\frac{\partial \overline{u'h'}}{\partial y}\right) \qquad (12)$$

where $C_{T_1} = \dfrac{1.32 + 7.5\,\pi/Re_\Lambda}{1 + 12.5\,\pi/Re_\Lambda}$ $\qquad C_{T_2} = \dfrac{1.165 + 12.5\,\pi/Re_\Lambda}{1 + 12.5\,\pi/Re_\Lambda}$

It should be noted that terms involving fluctuating densities (ρ') have been dropped in deriving Eqs. (1) - (12). This is generally permissible if the edge Mach number is below 4 or 5, as is usually the case for nosetip regions. However, if need be the dominant effects of density fluctuations can be included by defining a generalized Reynolds stress $R_{ij} = \overline{\rho u_i u_j}/\bar{\rho} = \overline{u_i' u_j'} + \overline{\rho' u_i' u_j'}/\bar{\rho}$. Once this is done the primary effect of density fluctuations is contained in a relatively unimportant diffusional term involving $\overline{\rho' v'}$, which can be related to $\overline{v' T'}$. The resulting formulation yielded good comparisons[6] with the measurements of Horstman et al.[7] in a boundary layer at $M_e = 7$.

Boundary conditions to Eqs. (1) - (12) are generally obvious: fluctuating quantities are zero at a solid wall or at the outer edge (if there is no free-stream turbulence). For numerical solutions, the equations are first transformed to the standard streamfunction coordinate, guaranteeing continuity and eliminating the normal velocity V. The transverse coordinate is also normalized by the edge value of the stream function (following Patankar and Spaulding),[8] so that additional mesh points need not be carried in the free stream to allow for boundary layer growth. For

many cases a uniform mesh in streamfunction coordinates is inadequate, and this is usually handled by further transforming the streamfunction. For example, for fully turbulent boundary layers a linear mesh in logarithm of the streamfunction is used. The finite-difference equations are solved with a block-tridiagonal Newton-Raphson or quasi-linearized technique.[1]

III. SMOOTH-WALL BOUNDARY LAYERS

The formulation that has just been presented has been tested against quite a few fully turbulent flows. Several of these were described previously,[1] and we shall not dwell on them here. Boundary layer flows for which satisfactory comparisons with available measurements have been obtained include the basic low speed flat plate turbulent boundary layer,[9] a "relaminarizing" boundary layer due to a favorable pressure gradient,[10] flat plate boundary layers with heat transfer at both low speeds[11] and high speeds,[7] and boundary layers with blowing.[12] Data from both low speed[13] and $M = 2.5$[14] plane mixing layers, and $M = 3$ axisymmetric wakes,[15] have also been satisfactorily reproduced.

The major emphasis of the current effort has involved boundary layer transition. One interesting aspect of our turbulence model is the fact that there is a minimum Reynolds number below which there cannot be a fully turbulent solution. This results from the Reynolds number dependence of dissipation. If the turbulent Reynolds number Re_Λ is decreased below about 40, the dissipation rate tends to increase (cf. Eq. 8) to such an extent that turbulence cannot be established. This corresponds to a momentum thickness $Re_\theta \cong 200$ in low speed flow, close to the linear stability limit, but to substantially higher values of Re_θ at high Mach numbers. This minimum Reynolds number can be closely related to transition in many high speed flows. To compute this minimum transition Reynolds number we simply specified a high level of free stream turbulence (3%) as a boundary condition, although the same result has also been obtained by artifically eliminating boundary layer growth. Figure 2 shows the distance Reynolds number at transition (defined as the location of

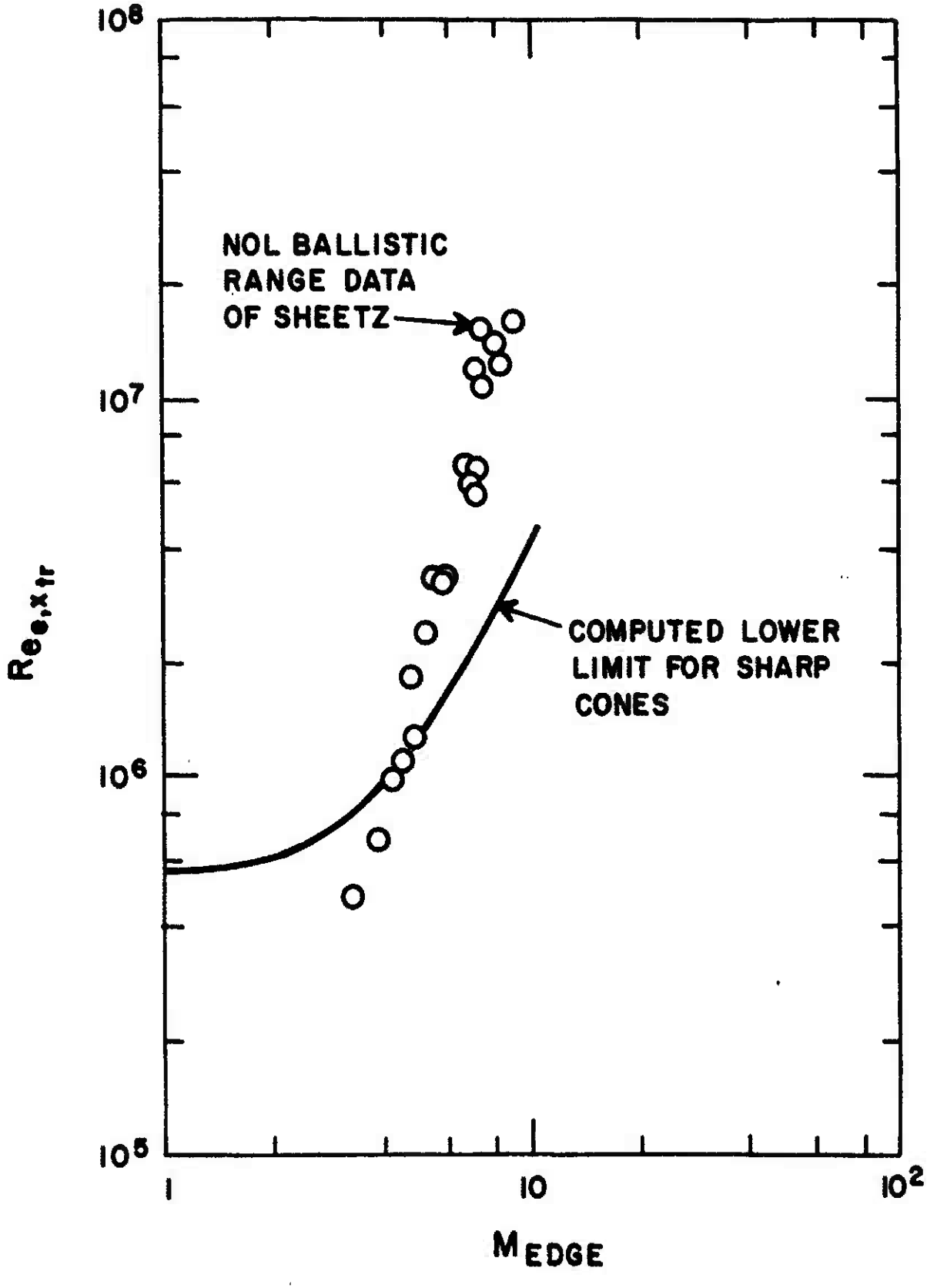

Fig. 2 Transition vs Mach Number on Cones

minimum skin friction) versus edge Mach number. Also included are the values obtained by Sheetz[16] from shadowgraph observations of nearly sharp slender cones. The computed trend is somewhat less pronounced than that observed by Sheetz, although the actual cone boundary layers may be influenced by entropy swallowing (the models had small but finite nose radii, whereas the calculations were performed for perfectly sharp cones).

Computations have also been performed in an attempt to investigate the role of free-stream turbulence on transition. We considered low speed flat plate cases, and started the calculations as a laminar boundary layer at small Re_θ. The free-stream turbulence was taken to be isotropic, with a sufficiently large scale size or small dissipation rate that the free-stream turbulence should decay negligibly over the distances to be considered. If the outer boundary conditions are identified with the free-stream turbulence, we then have a straightforward procedure for determining the transition location. However strong qualifications must be placed on the realism of this exercise. In most wind tunnels the free-stream fluctuations are largely acoustic rather than vortical, whereas the present formulation accounts only for the latter type. Also, wavelengths of free-stream turbulence are usually larger than the boundary layer thickness, violating an inherent assumption of all phenomenological turbulence models. It is not surprising then that computed transition is not in good agreement with wind tunnel results.* As Fig. 3 shows, the predicted transition is too soon except at the highest free-stream levels (where transition is dictated by the minimum Reynolds number considerations discussed above). And, until the response of a boundary layer to large scale pressure fluctuations can be theoretically treated, we cannot be optimistic about the prospects for adequately explaining these wind tunnel results.

---

* Wilcox[17] has recently obtained better agreement with such data, but his computations were apparently based upon extremely small, and non-realizable, length scales for the free-stream fluctuations.

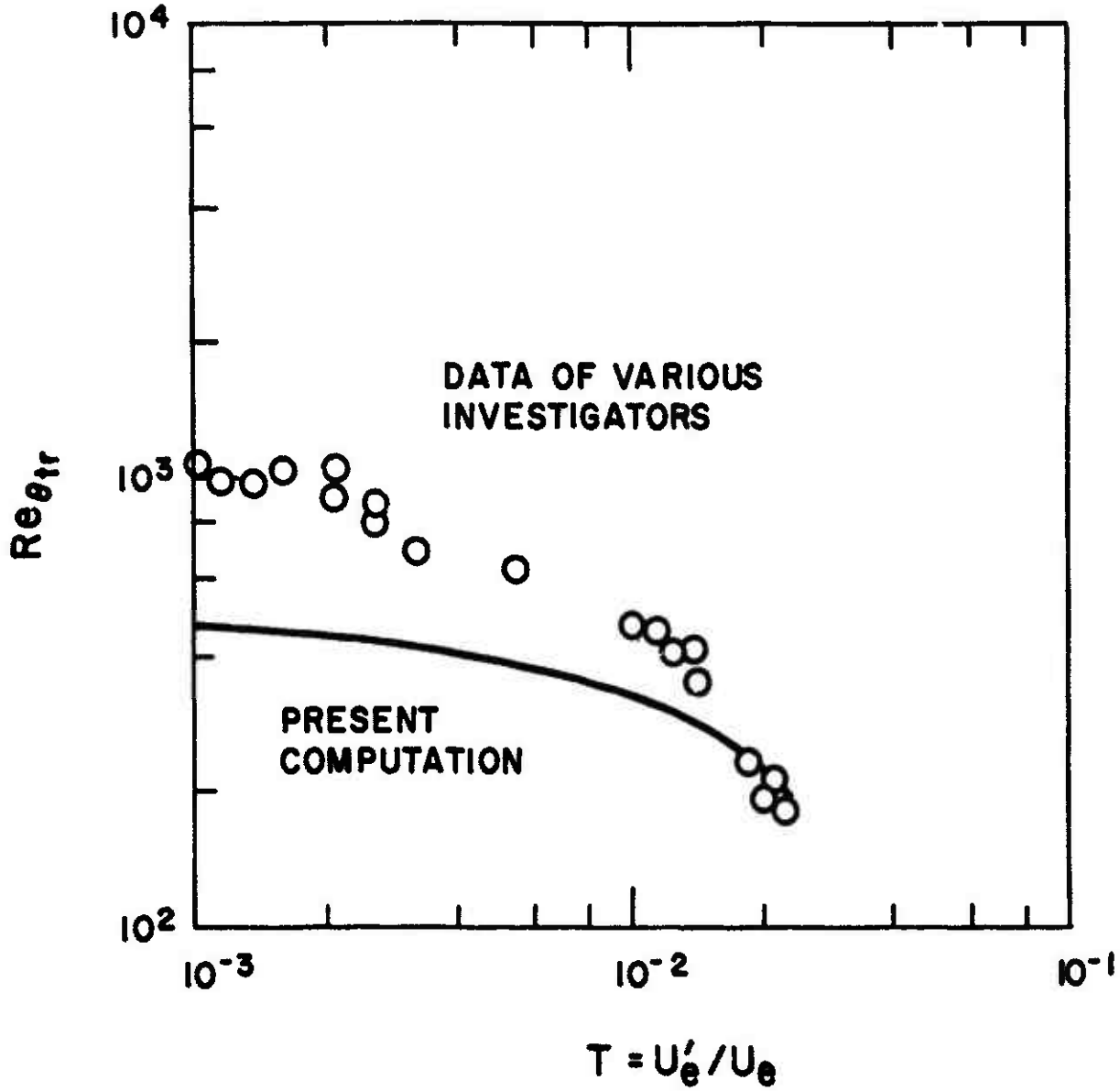

Fig. 3 Effect of Free-Stream Turbulence on Low Speed Transition

IV. MODEL FOR ROUGH-WALL BOUNDARY LAYERS

For actual reentry nosetips, transition is invariably the result of disturbances introduced by surface roughness elements. It is a classical result from low speed tests that roughness will have a significant effect on transition and on the subsequent turbulent boundary if the "roughness Reynolds number" $\rho U k/\mu$ is greater than about 100.[19] Anderson and Bartlett[20] have shown that this condition is usually exceeded on nosetips constructed of materials such as 3DQP and ATJ graphite. Furthermore an extensive laboratory simulation has been carried out by Aerotherm/Acurex Corporation under the PANT Program, and the experimental nosetip transition points have been correlated by Anderson[18] in the form

$$\frac{\rho_e U_e \theta}{\mu_e}\left(\frac{T_e}{T_w}\,\frac{k}{\theta}\right)^{0.7} = 215 \ .$$

The flow near an irregularly-shaped rough surface is undoubtedly quite complex, and one might envision several simplified models for this flow. If the roughness elements are typically large compared to boundary layer thicknesses, the flow might be approximated as that over a wavy wall. If the roughness elements were primarily two-dimensional - a series of trip wires, as in the experiment of Antonia and Luxton[21] - the flow might be treated as cavity flows between the elements. But for three-dimensional elements not taller than the boundary layer thickness, the most realistic model would appear to consider the wakes behind individual elements. It will be assumed that the flow approaching an element is attached and aligned parallel to the wall, even after having flowed past many upstream elements.

Through their wakes, roughness elements provide a distributed sink (due to drag) for mean momentum, and distributed sources for fluctuation energy and dissipation rate. To describe the distributed sources or sinks, we use a normal coordinate y whose origin is at the bottom of the elements. We shall idealize the rough surface as being made up of identical elements - all having the same height and shape, although the extension to a size distribution should be feasible. The shape is to be specified, and we shall consider simple shapes such as cones and hemispheres. Let k be the model roughness element height, let D(y) be the diameter of the element at height y (for $0 \leq y \leq k$), and let the average center - to - center element spacing be ℓ. We presume that the flow around an element at height y is approximately two-dimensional. That is, the flow around an element at height y looks like the flow around an infinite cylinder with diameter equal to D(y). This approximation will obviously be better for elements that are taller than they are wide, however, our results will probably not prove to be particularly sensitive to this two-dimensional approximation since disturbances are qualitatively similar in the near fields of two- and three-dimensional bodies.

The form drag on roughness elements should represent a sink term for the mean momentum equation. If C_D is the drag coefficient, the drag at height y (between $y - \delta y/2$ and $y + \delta y/2$) on a single element is

$$- \frac{1}{2} \rho U^2 C_D D(y) \delta y$$

To relate this to drag/unit volume, we note that there are ℓ^{-2} elements per unit surface area, so that the appropriate volume is $\ell^2 \delta y$ and the sink term for mean momentum is

$$- \frac{1}{2} \rho U^2 C_D D/\ell^2 \qquad (13)$$

This term is to be included in the right side of the mean momentum equation, Eq. (2). For the drag coefficient, we could specify $C_D = 1$, appropriate to infinite cylinders at local Reynolds numbers UD/ν above the Stokes flow regime. However, lower values such as 0.5 are more appropriate for finite elements such as cones and hemispheres, and the use of such a value provides a first-order correction for three-dimensional effects.

The fluctuations introduced by elements are more important for transition than is the mean drag. Visualization experiments on the flow behind isolated three-dimensional elements show their wakes to be generally oscillatory and quite complex. Mochizuki,[22] for example, showed that the wakes of isolated elements will actually be turbulent only at very high local Reynolds numbers, and that they undergo a sequence of oscillatory modes at lower Reynolds numbers. These modes include a horseshoe (streamwise) vortex, a "wing-tip" vortex shed off the top of the element and various other oscillations, but no evidence of a von Karman vortex street was seen. At very low Reynolds numbers the wake is completely laminar and non-oscillatory. This picture may be expected to be modified for distributed roughness elements, and it would appear to be quite difficult to write down an à priori specification for the fluctuations behind distributed roughness elements with great precision. However, these disturbances can be specified qualitatively, and the sensitivity to quantitative details can be evaluated in retrospect. Basically, except at very low Reynolds numbers, the velocity fluctuations behind an element should be proportional to the local flow velocity U

$$u' \sim Q_u U \tag{14}$$

where Q_u is a fractional number of order 10^{-1}. The kinetic energy per unit mass flux is u'^2, and the mass flux is approximately $\rho U D \cdot \delta y$.

Thus the kinetic energy created per unit volume is

$$(Q_u U)^2 \rho U D \delta y/(\ell^2 \delta y) = Q_u^2 \rho U^3 D/\ell^2 . \qquad (15)$$

A low Reynolds number cutoff to this term was also considered. Mochizuki's observations indicated no oscillations behind an isolated element for $Uk/\nu \lesssim 300$.[22] The presence of upstream elements would be expected to promote oscillations behind downstream elements, and the appropriate cutoff might occur at a value an order of magnitude lower for distributed roughness elements. However in practice any such cutoff is not critical. For very small roughness heights, k/δ is small except near a leading edge and the local flow velocity U is sufficiently small that the fluctuation source term of Eq. (15) is itself small. Thus we have not considered this effect in any detail.

In general, if fluctuations are created there should also be created a corresponding dissipation rate (Φ). If the size or wavelength of the oscillations is Λ, then the amount of dissipation/unit mass created is $\nu \overline{u'^2}/\Lambda^2$. The wavelength should be comparable to the diameter of the element, so that $\Lambda = Q_\Lambda D$ with $Q_\Lambda = 0(1)$. Then, following the same arguments leading to Eq. (15), the source term for the dissipation equation is*

$$\frac{Q_u^2}{Q_\Lambda^2} \rho U^3 \frac{\nu}{D\ell^2} \qquad (16)$$

In evaluating the role of this term in the calculations to be presented below, it was found that the term has no important effect on the development of fluctuations if $Q_\Lambda \geq 0.2$. However the term is given here for the sake of completeness.

---

* Note that the two-dimensional approximation breaks down here at the top of an element where $D \to 0$. In practice it is necessary to add a small fraction of the element height k onto D in Eq. (16).

The distributed source or sink terms given by Eqs. (13), (15), and (16) are the only ones that need be considered. If oscillations in the wake of an element are approximately isotropic, there should be no significant creation of the anisotropic components $\overline{u'v'}$, $S_{11} = \overline{u'^2} - 2/3q^2$, $S_{22} = \overline{v'^2} - 2/3\,q^2$. And, except in the Stokes flow regime, heat transfer to an element should be small and there should be no distributed source or sink terms in the equations for the thermal variables.

To our knowledge the model presented here is the first attempt to represent the disturbances introduced into a boundary layer by roughness elements. Using the Saffman two-equation turbulence model,[23] Wilcox[17] addressed the effect of roughness by making the wall boundary condition on their "pseudo-vorticity" (analogous to Φ/q^2) a function of wall roughness. While reasonable results were obtained for rough-wall transition, this approach does not address the source of the disturbances and, in fact, the disturbances were introduced as free-stream turbulence. In another study Merkle, Kubota and Ko[24] examined the effect of wall roughness on boundary layer stability. They estimated the increased mixing behind roughness elements using a wake description somewhat similar to that used here. This increased mixing alters the mean velocity profile and the stability characteristics; they then used the e^9 amplification ratio correlation[25] to relate amplification rate to transition location. However, form drag on the elements was not included, and examination of our calculations indicates that form drag has a much greater effect on the mean velocity than does the increase in mixing (Reynolds stress) due to fluctuations introduced by the elements. Also the e^9 correlation is based largely on wind tunnel data where free-stream turbulence must play a role and the analysis of Merkle et al makes no attempt to define the initial disturbances from a rough surface.

To obtain some verification of the validity of the model presented here for the effect of distributed wall roughness, calculations were performed for fully turbulent boundary layers. It was possible to compare the results with the measurements of Schlichting in flows over walls covered with idealized roughness elements of the type considered in our model - uniformly spaced spheres, hemispheres, cones, etc.[19] In performing these computations it was found that the primary effect of roughness is due to the form drag of the elements on the mean flow; the source terms for kinetic energy and dissipation rate are negligible compared to the normal production and dissipation terms in this fully turbulent regime. Three cases were considered, all at $U_e k/\nu \cong 10^3$: hemispheres with spacing ℓ of 2.5 and 5 base diameters and cones spaced 2.5 base diameters apart. Table I compares the local skin friction coefficients measured by Schlichting[19] with the results of the computations. Note that there is a slight overprediction, more pronounced in the case of hemispheres where a two-dimensional flow approximation is less likely to be valid. Details of the flow were found to be in good agreement with known results, not surprisingly since the primary effect of wall roughness on a turbulent boundary layer is simply to increase the wall shear. The mean velocity profile in the log region agreed satisfactorily with the well-known[19] $\ell n\,(y/k_s)$ behavior,* as shown in Fig. 4. Peak turbulent intensities increase with rough walls, but apparently can be completely scaled with the friction velocity U_τ as has been observed in many flows.[26]

---

* k_s is the equivalent sand-grain roughness height, defined for a general rough surface such that the wall shear is identical to that on a surface covered by sand grains of size k_s.

TABLE I

SKIN FRICTION COEFFICIENTS FOR
TURBULENT FLOW OVER ROUGH WALLS

Case	Schlichting Expt. $C_f \times 10^3$	Drag Coefficient in Calculations	Computed $C_f \times 10^3$
Smooth	~ 2.35	——	2.35
Spheres $\ell/d = 2.5$	~ 3.6 - 3.0	0.5	3.7
Spheres $\ell/d = 5.0$	~ 2.35	0.5	2.8
Cones $\ell/d = 2.5$	~ 3.4	1.0	3.8

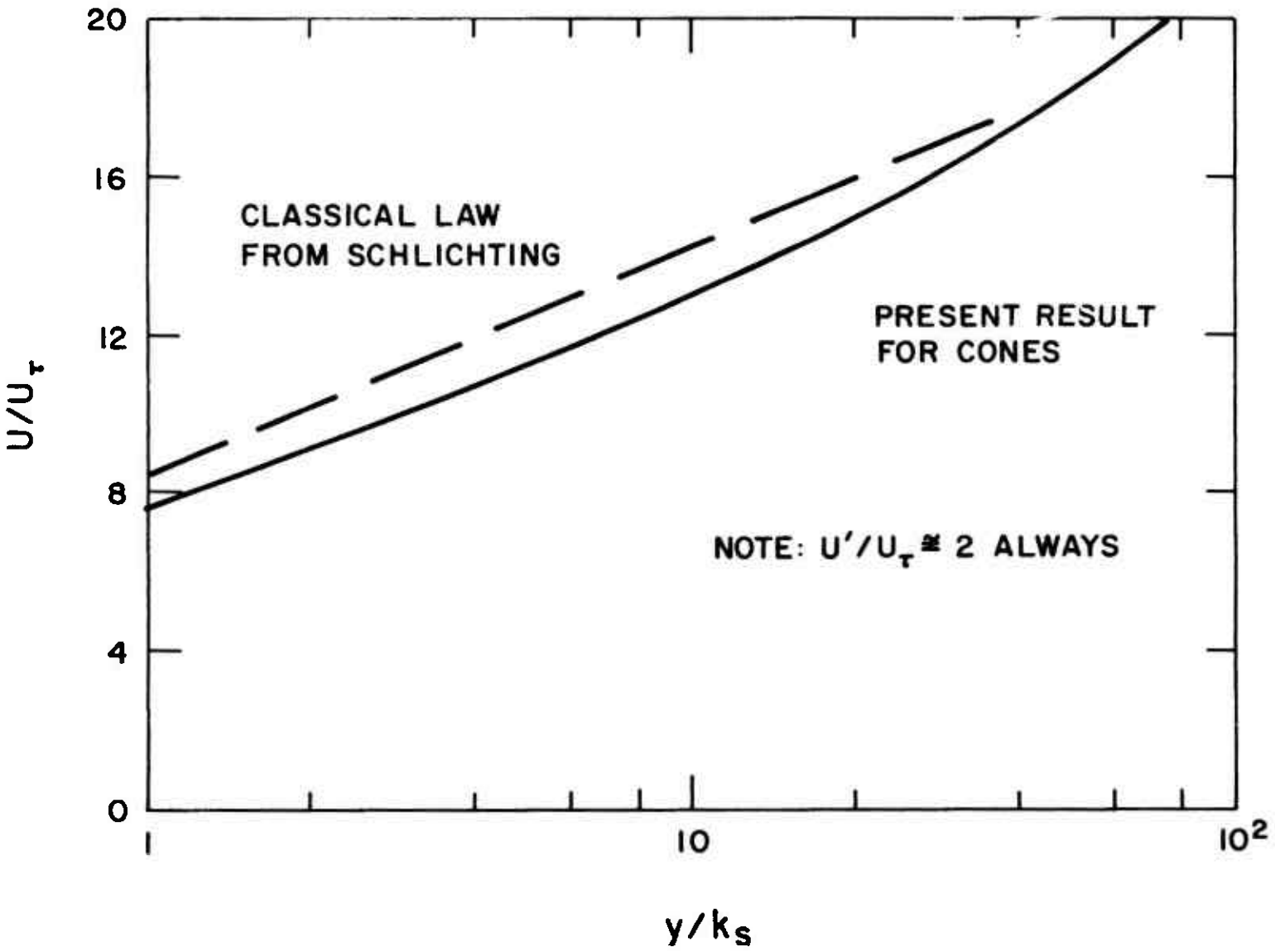

Fig. 4 Log Region Mean Velocity -
Turbulent Flow over Rough Wall

V. TRANSITION OVER ROUGH SURFACES

We now turn to the important issue of transition on rough surfaces, the immediate goal being to explain the measurements of Feindt[27] on sand paper roughened flat plates in low speed flows. It should be pointed out that the conclusions to be presented here apply to flat plates and not necessarily to blunt bodies. The flat plate boundary layer has zero thickness at the leading edge and is therefore smaller than any finite roughness height. On the other hand the boundary layer at the stagnation point of a blunt body has a nonzero thickness, so that sufficiently small roughness elements will always be well within the boundary layer. The present flat plate computations were initiated at a location very far upstream of transition, generally where $k/\delta = 1$, with a Blasius velocity profile and no turbulent intensity. The numerical results show a rapid initial increase in boundary layer thickness due to form drag of the roughness elements, and a buildup of fluctuation energy as a result of the distributed source terms. In all calculations to be presented here the free-stream intensity was set to zero, and the transition location was defined as the station of minimum wall shear.

In examining the sensitivity of the computed transition to the various inputs, it is clear that the dominant parameter is the height of the peaks of the elements. This height is not necessarily directly related to the equivalent sand grain size. The sand grain size is a measure of drag, which is weighted by the square of the local velocity, $U^2(y)$. On the other hand, the strength of the source term for fluctuations varies as $U^3(y)$. Since $U(y) \sim y$ (roughly), the peaks of the elements are more important for transition than for drag. In terms of the idealized specifications used here for rough surfaces, there are various combinations that yield the same equivalent sand grain size but give very different behavior for transition. For instance,

very tall and widely spaced elements could cause the same drag as shorter, more densely packed elements, but the taller elements produce a more rapid transition. Furthermore, cones would not be equivalent to hemispheres of the same height since there is little area near the apex of a cone. This behavior is illustrated in Fig. 5, where we show the streamwise variation of turbulent kinetic energy within the boundary layer for four roughness models all having the same equivalent sand grain size (the element spacing is varied to achieve this). The qualitative behavior of the kinetic energy will be discussed in detail shortly, but the transition location is seen to vary by a factor of three between short, closely-packed cones and tall, widely-spaced ones. Upon examination of photomicrographs of cross-sectional slices of rough surfaces,[18] it was decided that cones are probably not an ideal representation of actual roughness elements, and that hemispheres are probably much more appropriate. If spaced about two diameters apart, their height should be nearly equal to the equivalent sand grain height, and this type of roughness specification has been used for all calculations to be presented here. It might be appropriate to attempt to simulate an actual roughness distribution more precisely in future studies.

Figure 6 illustrates the development of the fluctuation energy as a function of distance and roughness Reynolds numbers. The nature of the behavior is rather interesting. At very small distances the boundary layer is thin, k/δ is appreciable, the elements encounter high local flow velocities, and the source term for kinetic energy (Eq. 15) is large. However, as the boundary layer grows downstream this source term becomes small and the fluctuation intensity decays by viscous dissipation and diffusion to the wall. Eventually, at $Re_x \simeq 10^5$ the boundary layer becomes sufficiently large ($Re_\theta \geq 200$) that the fluctuations can become amplified, leading to transition. It is interesting to note that the primary effect of roughness occurs well upstream, and isolated upstream roughness elements might have an effect similar to distributed roughness.

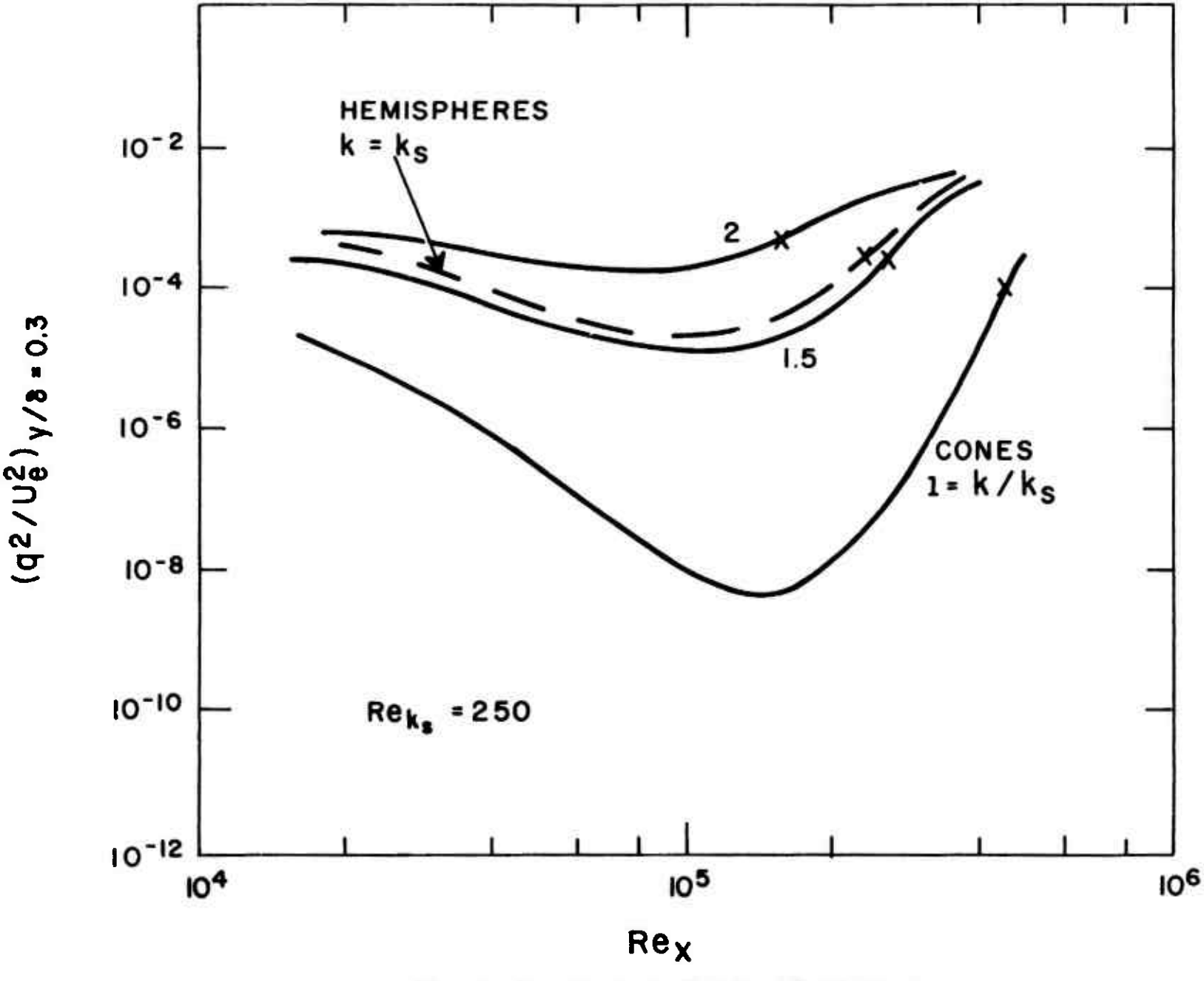

Fig. 5 Sensitivity to Height of Significant Peaks

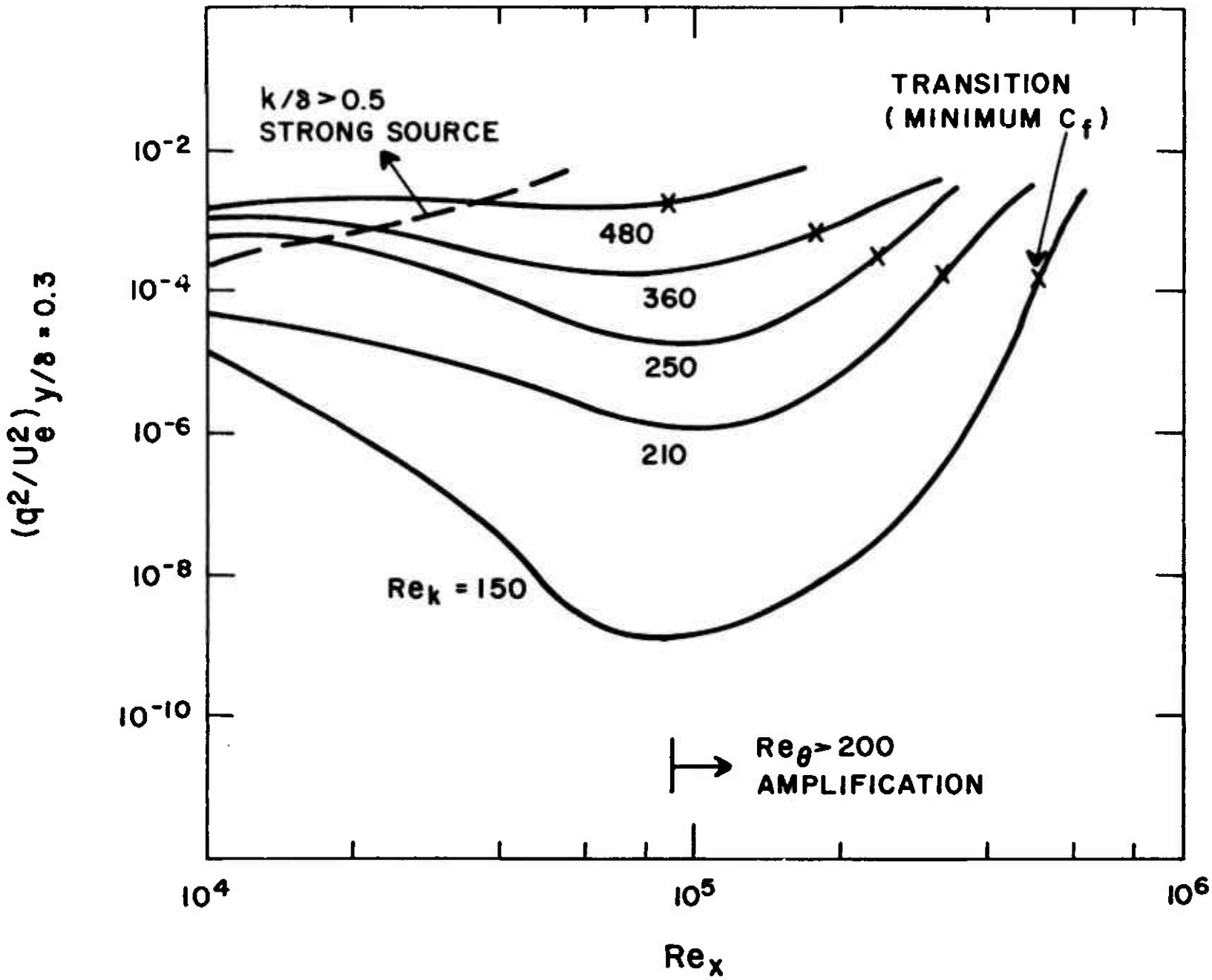

Fig. 6 Turbulent Intensity Development over Rough Walls

Figure 6 also sheds some light on the sensitivity of a transition prediction to the details of the model. Because the fluctuation energy experiences changes of several orders of magnitude (particularly at lower values of Re_k), factor of two uncertainties in the source term (e.g. in Q_u) are not critical. Furthermore, examination of the computations shows that the source term for the dissipation rate has no effect on the computed transition location as long as $\Lambda/D = Q_\Lambda \geq 0.2$. And, the form drag of the elements does not have an important effect on the laminar boundary layer beyond the far upstream region where $k/\delta \geq 0.5$.

The transition locations that result from the calculations of Fig. 6 are compared with the data of Feindt[27] in Fig. 7. Two curves are shown, for $k = k_s$ and $k = 0.8\, k_s$. This 20% difference reflects the minimum uncertainty in our current ability to characterize the actual surface. Agreement with Feindt's data is seen to be decent, although there appears to be some tendency to underpredict the transition distance at smaller roughness values. There the experiment was likely affected by free-stream turbulence, the data showing more scatter and almost exhibiting a double-valued character (we omitted Feindt's data points showing transition at $Re_x = 7 \times 10^5$ on a smooth wall). No attempt has been made to consider the combined effects of free-stream turbulence and roughness on transition.

Figure 8 presents the same calculations, but now plotted in terms of displacement thickness at transition and compared with a wider range of data.* Since displacement thickness is proportional to the square root of distance, this manner of presentation compresses the scales and the comparison is quite flattering.

A limited number of calculations have been performed for cases with pressure gradients, and one case at low Re_k is shown in Fig. 9.

---

*Comparable plots, in terms of momentum thickness rather than displacement thickness, are often used to correlate nosetip transition data.[18]

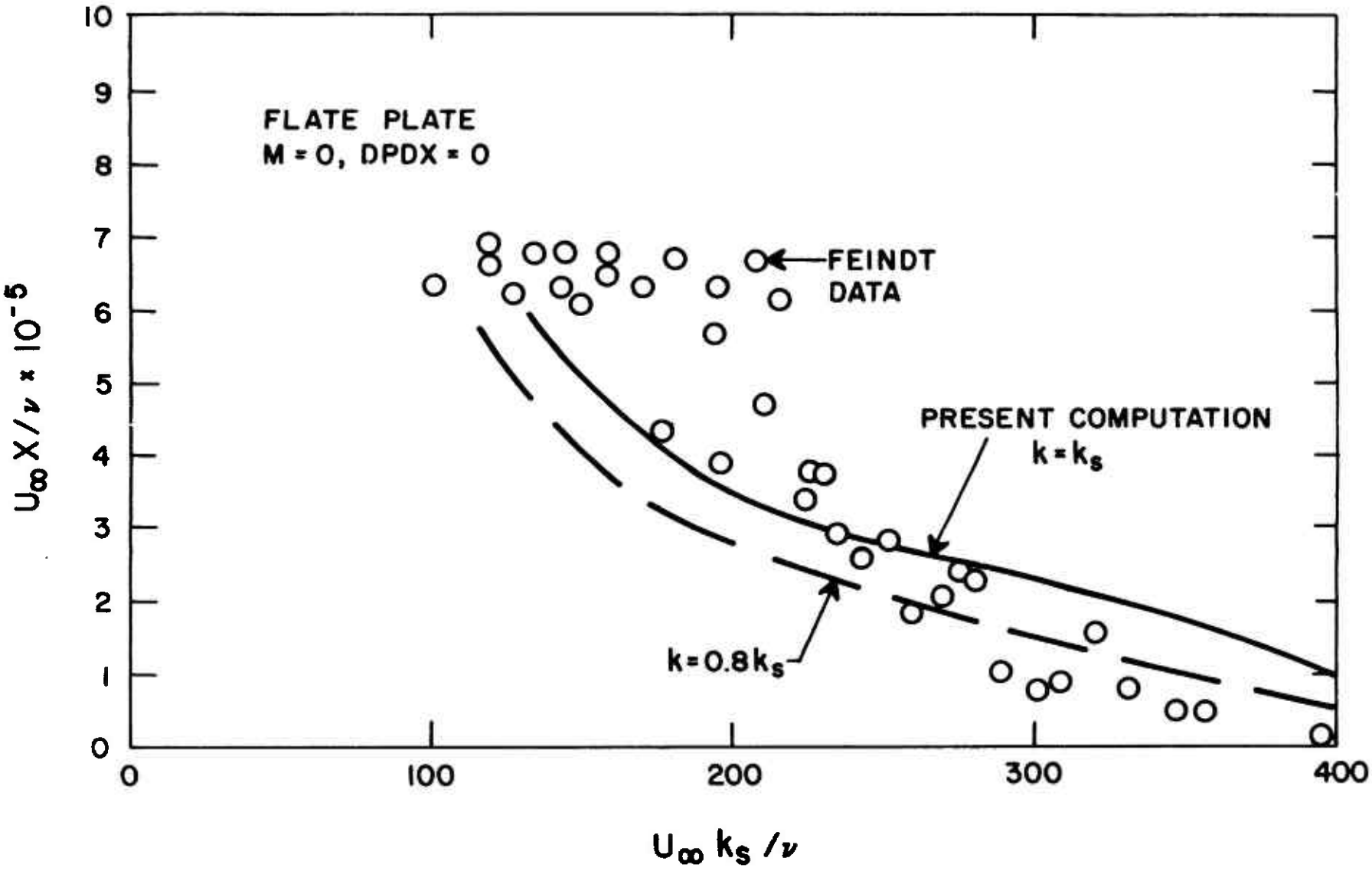

Fig. 7 Effect of Roughness on Transition

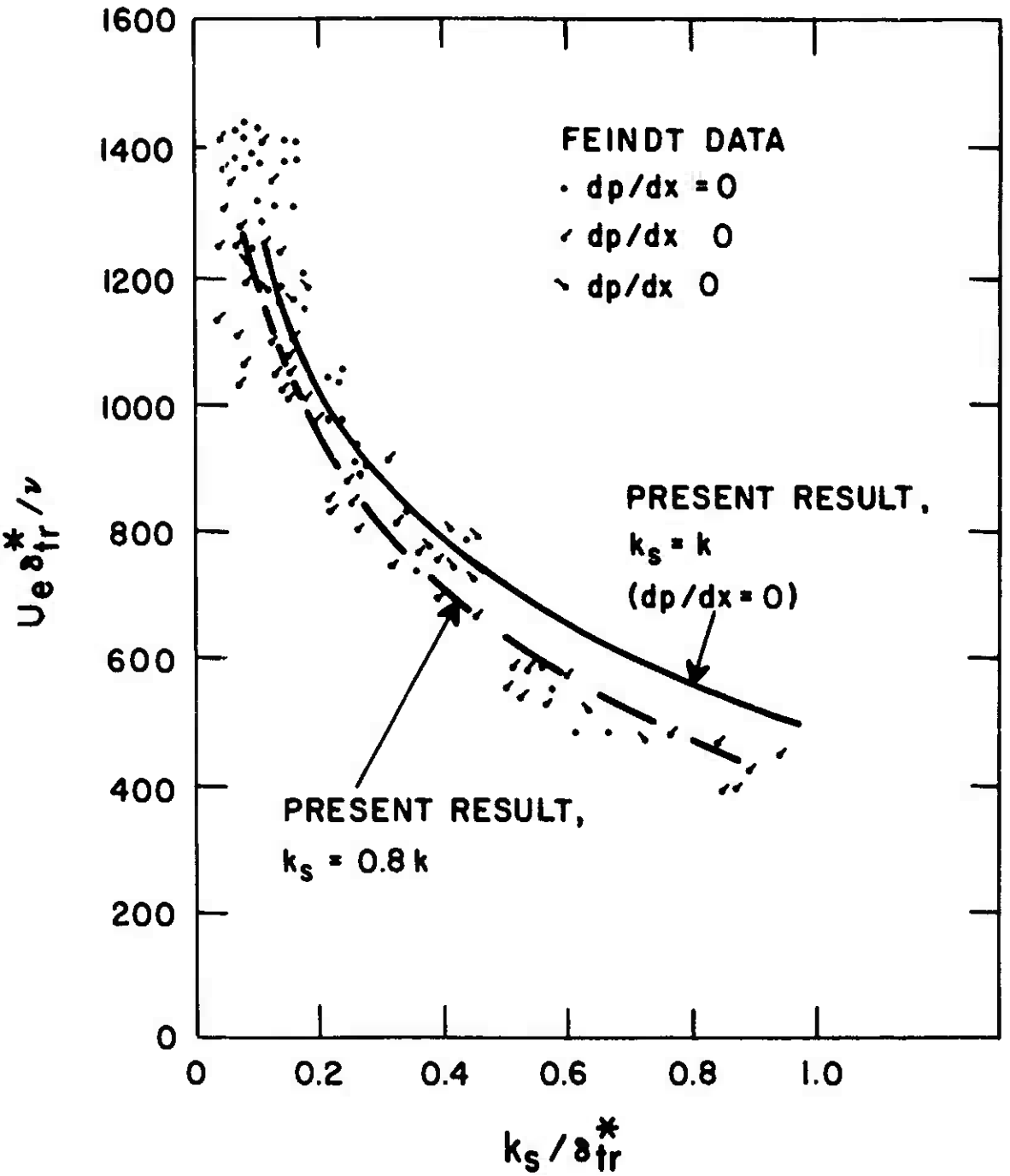

Fig. 8 Effect of Roughness on Flat Plate Transition

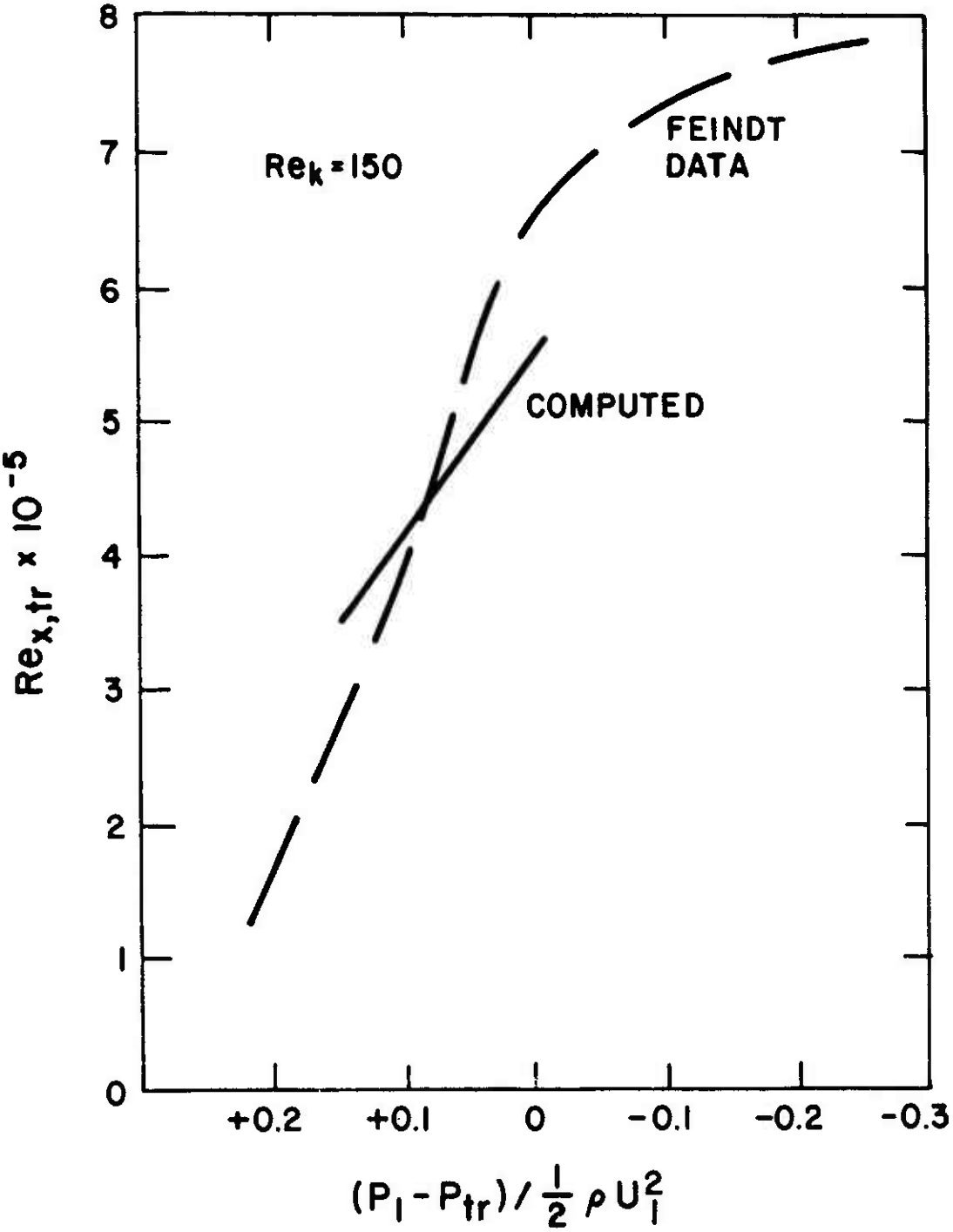

Fig. 9 Rough Wall Transition with Pressure Gradient

Adverse pressure gradients are plotted to the left, and they obviously promote more rapid transition. The computed trend is somewhat less than that indicated by Feindt, although it should be noted that his results are presented only in curve-fitted summary form and no data are available for individual cases with pressure gradients.

VI. SUMMARY

A theory based on the use of second-order moment equations is presented for transitional and turbulent boundary layer flows. The technique has yielded accurate predictions for various fully turbulent boundary layers, including those affected by pressure gradients and surface roughness. Although the model has yet to be adequately developed for treating transition induced by free-stream turbulence, a method is presented that addresses wall-roughness dominated transition. Using an idealized representation of distributed roughness elements, the disturbances introduced by the elements are described by wake relations and are handled as distributed source or sink terms in the governing relations for mean momentum and fluctuating energy. Calculations performed to date have been compared rather successfully with the transition measurements of Feindt[27] on sand paper-roughened flat plates in low speed flow.

The effects of roughness size and shape variations have been pointed out, and should be amenable to experimental verification. Representation of actual roughness distributions should be feasible in computations performed with this model. Further work is required to determine the behavior of transition on blunt bodies, and in high speed flows where the combined effects of compressibility, heat transfer, and entropy swallowing occur. Such efforts are currently underway, with the goal being the development of improved techniques for predicting transition on reentry body nosetips.

REFERENCES

1. Finson, M. L. et al., "Advanced Reentry Aeromechanics Interim Scientific Report", Report PSI TR-10, AFOSR-TR-74-1785, Physical Sciences Inc. (1974).

2. Finson, M. L., "A Second-Order Turbulence Model and its Application to Boundary Layers", in preparation.

3. Rotta, J., "Statistische Theorie nichthomogener Turbulenz", Zeitschrift fur Physik., 129, 547-572 (1951), and 131, 51-77 (1951).

4. Hanjalic, K. and Launder, B. E., "A Reynolds Stress Model of Turbulence and its Application to Thin Shear Flows", J. Fluid Mech., 52, 609-638 (1972).

5. Launder, B. E., Reece, G. J. and Rodi, W., "Progress in the Development of a Reynolds-Stress Turbulence Closure", J. Fluid Mech., 68, 537-566 (1975).

6. Lewis, P. F. and Finson, M. L., "Extension of Reynolds Stress Turbulence Models to High Speed Flows", to be published.

7. Horstman, C. C. and Owen, F. K., "Turbulent Properties of a Compressible Boundary Layer", AIAA J., 10, 1418-1424 (1972). Also Mikulla, V. and Horstman, C. C., AIAA Paper No. 75-119 (1975).

8. Patankar, S. V. and Spalding, D. B., Heat and Mass Transfer in Boundary Layers, Intertext Books, 1970.

9. Klebanoff, P.S., "Characteristics of Turbulence in a Boundary Layer with Zero Pressure Gradient", NACA Rept. 1247 (1956).

10. Launder, B. E., "Laminarization of the Turbulent Boundary Layer", M.I.T. Gas Turbine Lab. Rept. 77 (1964).

11. Verollet, E. and Fulachier, L., "Mesures de densités fe flux de chaleur et de tensions de Reynolds dans une couche limite turbulente over aspiration à la paror", Comtes Rendu Acad. Sci. Paris A 268, 1577-1580 (1969).

12. Wooldridge, C. E. and Muzzy, R. J., "Boundary-Layer Turbulence Measurements with Mass Addition and Combustion", AIAA J., 4, 2009-2016 (1966).

13. Patel, R. J., "An Experimental Study of a Plane Mixing Layer", AIAA J., 11, 67-71 (1973).

14. Ikawa, H. and Kubota, T., "Investigation of Supersonic Turbulent Mixing Layer with Zero Pressure Gradient", AIAA J., 13, 566-572 (1975).

15. Demetriades, A., "Turbulence Measurements in an Axisymmetric Compressible Wake", Phys. Fluids, 11, 1841-1852 (1968).

16. Sheetz, N. W., Jr., "Ballistics Range Boundary-Layer Transition Measurements on Cones at Hypersonic Speeds", in Viscous Drag Reduction, C. S. Wells, ed., Plenum Press, New York (1969).

17. Wilcox, D. C., "Turbulence-Model Transition Predictions for Blunt-Body Flows", DCW-R-03-01, AFOSR-TR-74-1714, DCW Industries (1974).

18. Anderson, A. D., "Boundary Layer Transition on Nosetips with Rough Surfaces", Aerotherm Acurex Corp. (1975).

19. Schlichting, H., Boundary Layer Theory, McGraw-Hill, New York, 1960.

20. Anderson, L. W. and Bartlett, E. P., "Boundary Layer Transition on Reentry Vehicle Nosetips with Consideration of Surface Roughness", TM-71-9, Aerotherm Acurex Corp. (1971).

21. Antonia, R. A. and Luxton, R. E., "The Response of a Turbulent Boundary Layer to a Step Change in Surface Roughness. Part 1. Smooth to Rough", J. Fluid Mech., 48, 721-761 (1971).

22. Mochizuki, M., "Smoke Observation on Boundary Layer Transition Caused by a Spherical Roughness Element", J. Phys. Soc. Jap., 16, 995-1007 (1961).

23. Saffman, P. G., "A Model for Inhomogeneous Turbulent Flow", Proc. Roy. Soc. A, 317, 417-433 (1970). Also Saffman, P. G. and Wilcox, D. C., AIAA J., 12, 541-546 (1974).

24. Merkle, C. L., Kubota, T., and Ko, D. R.S., "An Analytical Study of the Effects of Surface Roughness on Boundary-Layer Transition", Rep. No. 40, Flow Research, Inc. (1974).

25. Jaffe, N. A., Okamura, T. T., and Smith, A. M. O., "Determination of Spatial Amplification Factors and Their Application to Predicting Transition", AIAA J., 8, 301-308 (1970).

26. Townes, H. W. et al., "Turbulent Flow in Smooth and Rough Pipes", J. Basic Eng., 95, 353-362 (1972).

27. Feindt, E. G., "Untersuchungen uber die Abhangigkeit des Umschlages laminar-turbulent von der Oberflachenrauhigkeit und der Druckverteilung", Jahrbuch 1956 der Schiffbautechnischen Gesillschaft 50, 180-203 (1957).